Rapid analysis of legume root nodule development using confocal microscopy

Janine G. Haynes[1,2], Kirk J. Czymmek[2,3], Carol A. Carlson[1], Harita Veereshlingam[4], Rebecca Dickstein[4] and D. Janine Sherrier[1,2]

[1]Department of Plant and Soil Sciences, University of Delaware, Newark, DE 19717, USA; [2]Delaware Biotechnology Institute, Newark, DE 19711, USA; [3]Department of Biological Sciences, University of Delaware, Newark, DE 19716, USA; [4]University of North Texas, Department of Biological Sciences, Chestnut and Avenue C, Denton, TX 76203-5220, USA

Author for correspondence:
D. Janine Sherrier
Tel: +1 302 831 3550
Fax: +1 302 831 3447
Email: Sherrier@udel.edu

Received: *1 March 2004*
Accepted: *20 April 2004*

Summary

• A rapid method for detailed analysis of nodule formation has been developed.
• Inoculated root tissues were stained with SYTO 13, a cell-permeant fluorescent nucleic acid-binding dye, and visualized using confocal laser scanning microscopy (CLSM). Structures with high concentrations of DNA and RNA, such as plant cell nuclei and bacteria, labeled strongly. The autofluorescent properties of cell walls made it possible to use CLSM to visualize both plant and rhizobial structures and generate a three-dimensional reconstruction of the root and invading bacteria.
• This method allowed clear observation of stages and structures important in nodule formation, such as rhizobial attachment to root hairs, hair deformation, infection thread ramification, nodule primordium development and nodule cell invasion. Bacteroid structures were easily assessed without the need for fixation that might alter cellular integrity. Plant nodulation mutants with phenotypic differences in thread growth, cellular invasion and plant defense response were also documented.
• Multiple samples can be assessed using detailed microscopy without the need for extensive preparative work, labor-intensive analysis, or the generation of genetically modified samples.

Key words: bacteroid, CLSM (confocal laser scanning microscopy), *Medicago truncatula*, nitrogen fixation, nodule, rhizobia, SYTO, mutants (*nip*, *raz*, *sli*).

New Phytologist (2004) **163**: 661–668

© *New Phytologist* (2004) **doi**: 10.1111/j.1469-8137.2004.01138.x

Introduction

In nitrogen-limited conditions, rhizobia bacteria induce formation of nitrogen-fixing nodules on the roots of leguminous plants. A signaling dialogue between the host plant root and bacteria initiates formation of these nodules and results in significant gene-expression changes in both symbiotic partners within minutes to hours. Progression of the infection process can also be monitored at the cellular level, where both bacteria and plant undergo dramatic morphological changes. Bacteria bind to root hairs and induce reorientation of root-hair growth, resulting in hair deformation, curls and branches. At a site of high bacterial concentration on the hair surface, the plant forms an infection conduit termed an infection thread in which rhizobia grow, divide and infect the plant tissue. Concurrently, cells in the root cortex divide to give rise to a nodule meristem. Eventually, newly divided cells within the nascent root nodule develop infection threads, and bacteria are released from these threads into infection droplets within the host cell cytoplasm. The plant plasma membrane encompasses the infection droplets, maintaining the bacteria in a new compartment separate from the plant cytoplasm. The rhizobia and surrounding membrane, now called the symbiosome membrane, grow, divide and develop in concert, giving rise to hundreds of differentiated symbiosomes. For indeterminate nodules, such as those found on peas and *Medicago*, each symbiosome contains only one differentiated bacteroid. Biological nitrogen fixation occurs within the specialized symbiosome compartment formed by this complex developmental process. Several excellent reviews of nodule development are available (Mylona

et al., 1995; Bladergroen & Spaink, 1998; Cohn *et al.*, 1998; Schultze & Kondorosi, 1998; Stougaard, 2000; Limpens & Bisseling, 2003).

In recent years, the study of bacterial and plant mutants has facilitated the elucidation of the molecular mechanisms underpinning nodule development. Known plant and bacterial mutants or mutagenized populations of plants are evaluated for nodulation phenotypes using cytological methods. Defined mutants are then studied further to establish the exact cellular or tissue defect and the genetic lesion responsible for the mutant nodule phenotype. It is imperative therefore to utilize a high-resolution method to study the nodule phenotype in detail.

We present a method to perform detailed analysis of nodule phenotype without extensive preparatory work. In this study we show that all stages of wild-type nodule development can be visualized using this method. These observations were carried out at low magnification to observe changes in the overall root and at high magnification for observation of individual bacterial cells. Morphological differences between free-living rhizobia and bacteroids were also documented. Finally, the developmental defects of three plant nodulation mutants exhibiting abnormal infection thread development, apparent plant defense reactions, and delayed progression of infected cell formation are shown to demonstrate the utility of this technique for evaluating mutant nodule phenotypes.

Materials and Methods

Bacterial growth

For analysis of free-living bacteria, liquid cultures of *Rhizobium leguminosarum* bv. *viciae* 22 were grown in liquid tryptone yeast extract medium (TY) + kanamycin (50 μg ml^{-1}) to an optical density of 0.6 at 28°C and 260 r.p.m.

Nodule production

Medicago truncatula A17 and mutants, and *Pisum sativum* L. cv. Early Alaska were grown in aeroponic growth chambers and inoculated with *Sinorhizobium meliloti* 2011 (Meade *et al.*, 1982) or *R. leguminosarum* bv. *viciae* 3841 (Wood *et al.*, 1989), respectively, using established methods (Catalano *et al.*, 2004; Vedam *et al.*, 2004). Infected *Medicago* and pea tissues were harvested 2, 3, 9, 20, 25 and 31 days post-inoculation (dpi) to evaluate stages of normal nodule development. *Medicago truncatula* mutants were harvested at 9, 13, 20 or 25 dpi for assessment of nodule phenotype.

Tissue staining and confocal light microscopy

For analysis of early nodule development, inoculated roots were harvested into 50 mM PIPES buffer pH 7.0. Segments of root where root-hair proliferation or deformation was observed were cut away from the root systems, transferred to 4% formaldehyde in 50 mM PIPES, and vacuum infiltrated 3 × 30 s, venting completely in between. Roots were fixed with rotation for 45 min at room temperature, rinsed 2 × 5 min with 50 mM PIPES buffer, and transferred to ice-cold 80% ethanol. Roots in ethanol were stored at −20°C for 45 min, then rinsed 2 × 5 min with 50 mM PIPES buffer. Roots were moved to fresh PIPES buffer and cut by hand into cross-sections with a double-edged razor blade. Root sections were stained with 1 μl ml^{-1} SYTO 13 (Molecular Probes, Inc., Eugene, OR, USA) in PIPES for 15 min.

For evaluation of mature nodules, *M. truncatula* and pea nodules were harvested into 80 mM PIPES buffer and bisected longitudinally using a double-edged razor blade. Cut nodules were stained in 80 mM PIPES with 1 μl ml^{-1} SYTO 13 for 15 min.

Bacteroids were commonly released from nodule cells during the process of dissection, staining and subsequent transfer to the slide; these released bacteroids frequently accumulated at the coverslip in close proximity to nodules and were readily imaged without the need for biochemical isolation.

To stain free-living bacteria, mid- to late-log cultures of *R. leguminosarum* bv. *viciae* 22 in TY were incubated with 1 μl ml^{-1} SYTO 13 for 15 min at room temperature. Treated culture (25 ml) was concentrated with a 0.2 μm Stericup filtration unit system.

Stained root sections, nodule halves and bacterial samples were transferred to a Laboratory-Tek II chambered #1.5 coverglass system (Nalge/Nunc International, Naperville, IL, USA) in a small volume of the staining solution, and gently covered with a glass coverslip (No. 1 coverslips, 18 mm circles) to minimize sample movement and position the sample closer to the coverslip.

Confocal images were acquired on an inverted Zeiss LSM 510 NLO laser-scanning microscope (Carl Zeiss, Inc., Germany) using a Zeiss ×10 Plan-Apochromat lens (NA 0.45), ×20 Plan-Apochromat lens (NA 0.75), ×40 C-Apochromat (NA 1.2), or ×100 Plan-Neofluar (NA 1.3) objective lens. Data acquisition of SYTO 13 only used the 488 nm laser line of a 25 mW Argon laser (LASOS, Ebersberg, Germany) with a 505LP emission filter. Multi-channel images of SYTO 13 and autofluorescence were acquired in fastline-switch mode using the 488 and 543 nm Helium Neon laser lines (LASOS) with the 500–550 band-pass and 560 long-pass emission filters, respectively. Images were captured as single optical sections (2-D) or as a z-series of optical sections (3-D). For renderings, 3-D data sets were displayed as single maximum-intensity projections generated using Zeiss LSM software ver. 3.2. The SYTO 13 fluorescence was depicted in green and the plant autofluorescence in blue.

Results

Wild-type nodule formation

Medicago truncatula A17 and *P. sativum* cv. Early Alaska roots were inoculated with wild-type *S. meliloti* or *R. leguminosarum*

bv. *viciae*, respectively, and the progression of nodule development was studied in detail using the fluorescent nucleic acid-binding dye SYTO 13 and confocal laser scanning microscopy (CLSM). Tissues were collected in a developmental time course so that all stages of nodule formation could be observed and documented. For early stages of development, inoculated roots were stained directly after harvest (not shown), or subjected to a short fixation process before staining. Epidermal preservation and final images were superior if the roots were fixed before staining, and those results are shown in Fig. 1. The entire fixation and staining process took approx. 2 h. Nodules and bacteroids required no fixation step, and were processed for microscopy in < 30 min.

At 2 dpi rhizobia were bound to the epidermal surface of the root, and root hairs displayed characteristic features of early nodule development including root-hair deformation and curling (Fig. 1a). At the same time point, inner cortical cells opposite the xylem pole of the root stele reactivated the cell cycle, giving rise to a new meristem (Fig. 1b). Sites of nodule formation were distinguished by wide meristems in the root inner cortex (Fig. 1c). By 3 dpi bacteria invaded the plant tissue through root-hair infection threads (Fig. 1d). At later time points bacteria invaded individual plant cells, occupying a large portion of the cell volume (Fig. 1e). In these mature tissues, remnant infection threads were visible (Fig. 1f) and individual undifferentiated bacteria were distinguishable within the threads (Fig. 1g). All stages of infected cell development were observed within one medial longitudinal view of a mature nodule (Fig. 1h). The persistent meristem, prefixation zone, interzone and nitrogen-fixation zone were easily distinguished within mature nodules.

Bacteroid differentiation

Development of the nodule is facilitated by extreme morphological differentiation of both plant and microbe. Plants manifest these changes by the development of a nodule, while bacteria alter their morphology within infected cells of the host plant. Free-living rhizobia are rod-shaped microbes, and this shape was distinguished clearly by staining bacteria in liquid culture and using CLSM (Fig. 2a). Branched and enlarged bacteroid shapes were readily observed in bacteria released from cut nodules (Fig. 2b) or in bacteroids isolated from nodule tissue (not shown).

Plant nodulation mutants

To demonstrate the utility of this method for distinguishing phenotypic differences in nodulation mutants, nodules from three *M. truncatula* mutants were harvested and observed. Two mutants, *nip* and *sli*, were originally identified in a screen for early nodulation mutants (R.D. and colleagues, in preparation) and a third mutant, *raz*, was identified as a metal hyperaccumulator (Ellis *et al.*, 2003). A wide range of nodule phenotypic differences was documented using SYTO 13 and CLSM. Aberrant infection thread formation and growth was observed in infected *nip* roots at 13 and 25 dpi, indicating a defect in the early stages of nodule formation (Fig. 3a,b). In this mutant the prefixation zone of the nodule was enlarged, and infection threads were thickened and branched in comparison to threads in wild-type nodules (Fig. 1f,h). In addition, the autofluorescence in the root was much more intense and widely distributed than in the wild-type nodule, suggesting induction of a plant defense response in the *nip* nodules. A second mutant, *sli*, formed small nonfixing nodules and very few large nodules. In the rarely occurring large nodules of *sli*, rhizobia invaded plant host cells (Fig. 3c), and the contents of vacuoles within uninfected intervening cells in the nitrogen-fixation zone fluoresced brightly, suggesting induction of a plant defense response (Fig. 3d). By contrast, uninfected cells within the nitrogen-fixation zone of wild-type nodules did not fluoresce (Fig. 1h). In *raz*, a zinc-hyperaccumulating plant (Ellis *et al.*, 2003), a more subtle nodule phenotype was observed: cells were invaded but the vacuoles in infected cells often remained large and bacterial occupancy remained low throughout cellular development (Fig. 3e,f), indicating a possible block or delay in infected cell maturation. In contrast, enlarged infected cells in wild-type nodules contained one or more small vacuoles and abundant bacteroids filled the cytoplasm of the cells (Fig. 1e,f,h).

Discussion

Formation of nitrogen-fixing root nodules is a complex biological process characterized by dramatic morphological changes in the host plant and rhizobia. Here we describe a simple and rapid microscopy method to assess the progression of root nodule development (large numbers of samples can be processed in 30 min). This approach is especially attractive for nodule evaluation because it does not require time-consuming genetic transformation or labor-intensive sectioning, and is compatible with conventional fluorescence microscopes or high-resolution 3D imaging with confocal microscopy. The ease of the method allows for observation of high numbers of infected roots and nodules and meaningful statistical analysis of observed phenotypes.

In this study, fresh or fixed plant tissues and bacterial cells were stained with SYTO 13, a cell-permeant fluorescent nucleic acid-binding dye, and imaged using CLSM. This dye has been used previously in diverse studies to examine environmental bacterial samples (Guindulain *et al.*, 1997), to analyze bacteria by flow cytometry (Frey, 1995; Comas & Vives-Rego, 1997, 1998; Mason *et al.*, 1998), and to characterize nuclear changes in various animal tissues after treatment with toxins (Cook & Van Buskirk, 1997; Holmstrom *et al.*, 1998; Pulliam *et al.*, 1998). It is a particularly useful stain for studying nodulation because it stains both concentrated plant DNA and rhizobial cells. In our hands, we found that classical

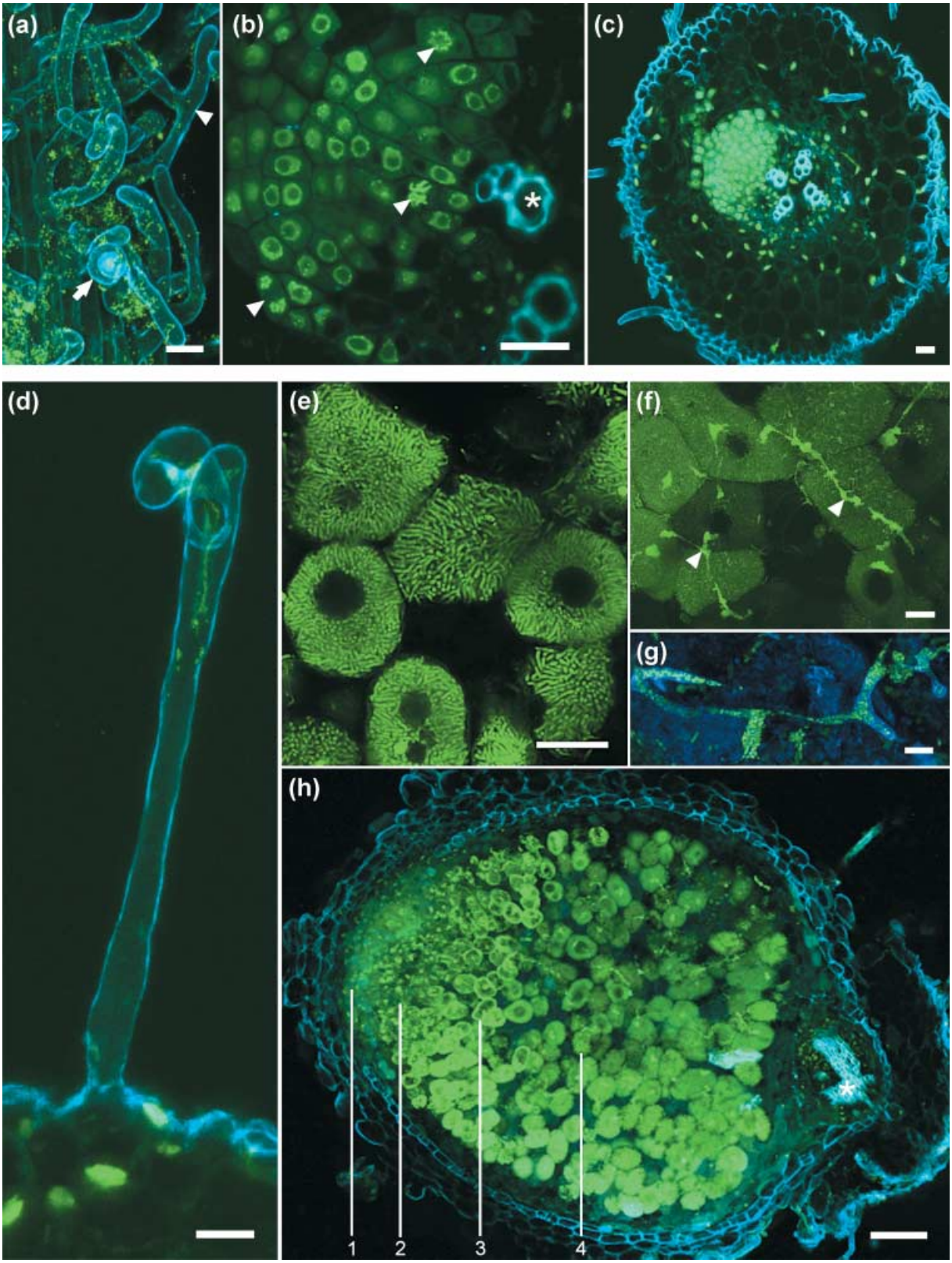

Fig. 1 Development of wild-type *Medicago truncatula* and *Pisum sativum* root nodules visualized using confocal microscopy. (a) *M. truncatula* A17 at 2 d post-inoculation (dpi) with *Sinorhizobium meliloti* 2011. Root hairs are branched (arrowhead) and curled (arrow). Bacterial cells are shown in green. Bar, 20 μm. (b) Nascent nodule meristem near the stele of a *Medicago* root at 2 dpi. *, Vessel member; arrowheads, condensed chromatin in meristematic cells. Bar, 20 μm. (c) Cross-sectional view of *Medicago* root forming a nodule meristem (highlighted in green) at 2 dpi.

DNA-binding dyes such as DAPI and Hoechst 33342 were best suited for labeling plant nuclei (and some nonspecific staining of plant cell walls), with only very modest labeling of rhizobia. Others have shown the utility of using DAPI in combination with acridine orange for labeling root nodules, with most of the rhizobial staining derived from acridine orange (Dudley *et al.*, 1987). DAPI, which specifically binds the minor groove of DNA in AT-rich regions (Trotta & Paci, 1998), labels the nucleoid of the bacteria, while acridine orange and SYTO 13 label cytoplasmic RNA as well as nucleoid DNA. While the combination of DAPI and acridine orange yields excellent micrographs, SYTO 13 has several advantages for the applications outlined in this paper. First, the extinction coefficient (EC) and quantum yield (QY), commonly used as measures of fluorophore brightness, are significantly different for SYTO 13 (EC = 74 000 m^{-1} cm^{-1}, QY = 0.40) and acridine orange (EC = 27 000 m^{-1} cm^{-1}, QY = 0.20) (www.probes.com). These values equate to SYTO 13 being four to five times brighter than acridine orange. Acridine orange's pH sensitivity can be problematic in certain situations where specificity is a concern, and with acidic cellular compartments such as vacuoles and symbiosomes. Lastly, for multiple probe experiments on root nodules, use of acridine orange may complicate imaging because of its spectral properties: it produces a green emission when bound to DNA and a far-red emission (approx. 650 nm) when bound to RNA. A combination of the above-mentioned factors clearly provides impetus for utilizing a bright, highly specific, permeable probe with narrow spectral emission characteristics for root nodule studies, as is the case with SYTO 13.

Many stages of nodule development were documented in wild-type plant–bacterium interactions. To explore the usefulness of this method in distinguishing perturbations in nodule development, we evaluated the major phenotypic changes in three *M. truncatula* mutants. Evaluation of inoculated plant mutants revealed clear differences in the developmental progression of nodule formation compared with wild-type plants. Defects in infection thread formation and growth, disruption of infected cell development, and apparent plant defense responses in nodules were observed. More detailed molecular genetic, biochemical and morphological studies of these mutants are currently under way by several groups (R. Dickstein *et al.*, in preparation; D.J. Sherrier *et al.*, unpublished).

Other microscopy techniques have been adapted to study nodule formation. The use of phase-contrast microscopy, bacteria or plants transformed with cytological markers (e.g. gus, gal, gfp), and conventional stains have all proven successful means of studying nodule formation. For example, Fahraeus (1957) presented a technique utilizing a glass slide chamber for root growth and plant inoculation. This approach was used in concert with phase microscopy to monitor the developmental progression of clover root infection by *Rhizobium*. However, in general, transmitted light techniques are restricted with regard to specificity, and resolution can be degraded in thick tissues such as roots. Truchet *et al.* (1989) developed methods using conventional stains to distinguish between nascent nodules and lateral root meristems. Molecular approaches for galactosidase- or glucuronidase-tagged rhizobia have also been utilized to monitor the progression of symbioses (Boivin *et al.*, 1990; Wilson *et al.*, 1995). More recently, Gage *et al.* (1996) transformed rhizobia with a variant of the green fluorescent protein and analyzed the early events in alfalfa infection by *S. meliloti*. This approach has been widely adopted for the study of nodule formation. For example, this method was recently put to elegant use in a study of Nod factor perception where the transformed plant was also tagged with the fluorescent protein DS RED (Limpens *et al.*, 2003).

Each of the aforementioned techniques is a very powerful tool, and has provided critical data on aspects of root nodule development. Green fluorescent protein, in particular, holds great promise, especially for *in vivo* studies. However, fluorescent proteins require genetically tractable organisms and must be performed for each mutant to be studied, while SYTO 13 can be applied to any mutant. Also, fluorescent protein studies of nodule development have most often been restricted to either host or pathogen, hence other structures (cell walls, nuclei, vascular tissue, meristem) must be contrasted using other methods. Specific modifications of our technique, used in conjunction with the CLSM method described herein, could be readily exploited to study nodule formation with fluorescent proteins. For example, fluorescent protein spectral variants that are compatible with SYTO 13 could be used to document additional relevant molecules in the host and/or symbiont simultaneously. In addition, this method can be applied to cryosections and immunofluorescence of fixed tissues when antibodies are required for protein localization studies.

With our method, infection thread initiation, growth and morphology can be observed in great detail. In addition, infected cell formation and development can be ascertained by noting the degree of cellular occupancy and bacteroid

Fig. 1 continued Bar, 20 μm. (d) High-magnification image of a curled root hair forming the classic 'shepherd's crook' on *Medicago* with an infection thread growing toward the root at 3 dpi. Bar, 20 μm. (e) High-magnification image of *Medicago* nodule cells in the nitrogen-fixation zone at 9 dpi. Individual bacteroids are clearly visible. Bar, 20 μm. (f) Infected cells in the fixation zone of a mature *Medicago* nodule with remnant infection threads at 25 dpi. Arrowheads, remnant infection threads. Bar, 20 μm. (g) High-magnification image of a branching infection thread in a mature pea nodule at 31 dpi. Note the cell wall of the infection thread (blue) and the undifferentiated bacterial cells (green) inside the infection thread. Bar, 5 μm. (h) Longitudinal section of a mature *Medicago* root nodule at 20 dpi. Regions of a mature nodule visible using confocal microscopy: 1, nodule meristem; 2, prefixation zone; 3, interzone; 4, nitrogen-fixation zone. *, Stele of root. Bar, 100 μm.

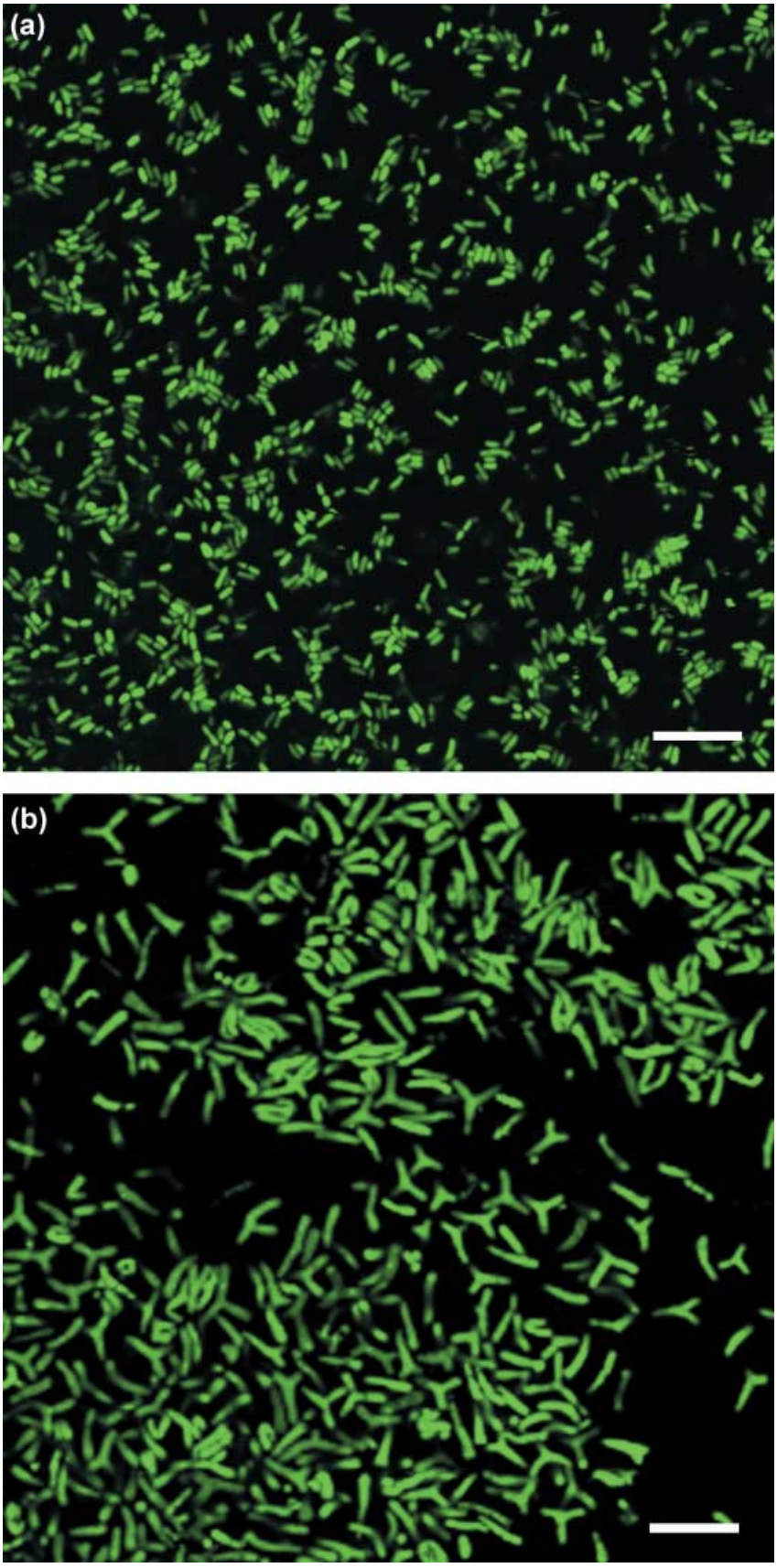

Fig. 2 Rhizobial cells stained with SYTO 13. (a) Free-living *Rhizobium leguminosarum* bv. *viciae* cells grown in liquid culture. (b) Differentiated bacteroids of *Sinorhizobium meliloti* 2011 released from mature root nodules at 25 dpi. Bars, 10 μm.

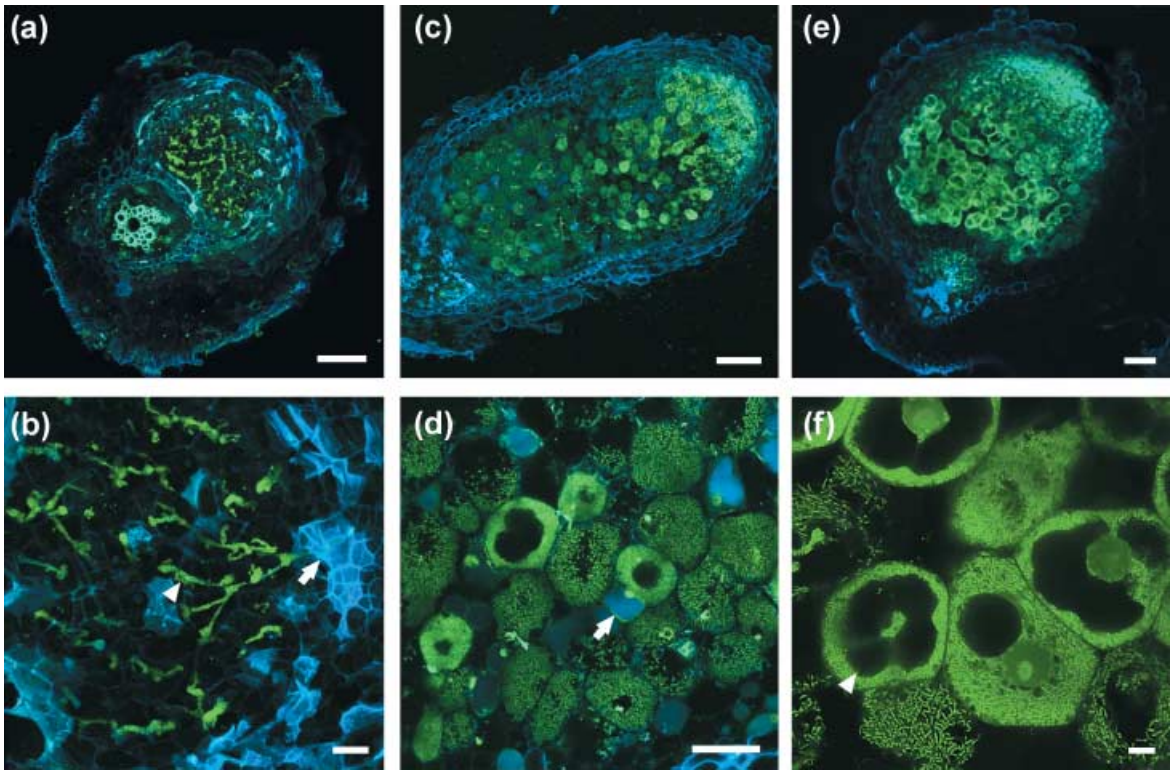

Fig. 3 Assessment of nodule phenotype in mutant *Medicago truncatula* using confocal microscopy. Longitudinal sections of mature nodules stained with SYTO 13. (a) Abnormal nodule structure formed by *Medicago nip* mutant at 13 dpi. The mutant forms abnormally small nodules with numerous infection threads. Bar, 100 μm. (b) High-magnification view of *nip* nodule structure at 25 dpi. The mutant exhibits a proliferation of aberrant infection threads (green) and accumulations of autofluorescent compounds (blue) in cells surrounding them. Bar, 20 μm. (c) Rarely occurring nodule formed by *Medicago sli* mutant at 25 dpi. Mature nodule has relatively normal morphology but exhibits autofluorescence in certain cells of the fixation zone. Bar, 100 μm. (d) High-magnification image of *sli* nodule cells in fixation zone at 25 dpi. Cells in the nitrogen-fixation zone have normal occupancy but surrounding cells fluoresce in a potential defense response. Bar, 20 μm. (e) Nodule formed by *Medicago raz* mutant at 20 dpi. Nodule cells in the fixation zone exhibit a persistent large central vacuole. Bar, 100 μm. (f) High-magnification image of *raz* nodule cells at 9 dpi. Cells in the nitrogen-fixation zone have low nodule occupancy compared with wild-type nodules, and large vacuoles persist in many of the infected cells. Bar, 20 μm.

morphology. Bacterial differentiation during nodule development can be monitored within intact nodule tissues or in bacteroids released or purified from root nodules. This method is particularly useful for screening mutants affected in one of these fundamental processes of nodule formation. We expect that this approach will be of great benefit to researchers exploring legume root nodule development, as it has greatly accelerated our own ability to assess an array of mutants for nodule development.

Acknowledgements

We thank C. Catalano for help with preliminary studies. This work was supported by USDA NRI grants # 2001-35318-10915 and # 2001-35311-10161 to D.J.S., a University of Delaware Life Science Scholar Fellowship to C.C., The University of Delaware Research Foundation, NIH BRIN #RR16472-02 to the Delaware Biotechnology Institute, and University of North Texas Faculty Research Grants to R.D.

References

Bladergroen MR, Spaink HP. 1998. Genes and signal molecules involved in the rhizobia–Leguminoseae symbiosis. *Current Opinion in Plant Biology* **1**: 353–359.

Boivin C, Camut S, Malpica CA, Truchet G, Rosenberg C. 1990. *Rhizobium meliloti* genes encoding catabolism of trigonelline are induced under symbiotic conditions. *Plant Cell* **2**: 1157–1170.

Catalano CM, Lane WS, Sherrier DJ. 2004. Biochemical characterization of symbiosome membrane proteins from *Medicago truncatula* root nodules. *Electrophoresis* **25**: 519–531.

Cohn J, Day RB, Stacey G. 1998. Legume nodule organogensis. *Trends in Plant Science* **3**: 105–110.

Comas J, Vives-Rego J. 1997. Assessment of the effects of gramicidin, formaldehyde, and surfactants on *Escherichia coli* by flow cytometry using nucleic acid and membrane potential dyes. *Cytometry* **29**: 58–64.

Comas J, Vives-Rego J. 1998. Enumeration, viability and heterogeneity in *Staphylococcus aureus* cultures by flow cytometry. *Journal of Microbiological Methods* **32**: 45–53.

Cook JR, Van Buskirk RG. 1997. A double-label technique that monitors sulfur mustard damage to nuclei and mitochondria of normal human epidermal keratinocytes *in vitro*. *Toxicologic Pathology* **25**: 481–486.

Dudley ME, Jacobs TW, Long SR. 1987. Microscopic studies of cell divisions induced in alfalfa roots by *Rhizobium meliloti*. *Planta* **171**: 289–301.

Ellis DR, López-Millán AF, Grusak MA. 2003. Metal physiology and accumulation in a *Medicago truncatula* mutant exhibiting an elevated requirement for zinc. *New Phytologist* **158**: 207–218.

Fahraeus G. 1957. The infection of clover root hairs by nodule bacteria studied by a simple glass slide technique. *Journal of General Microbiology* **16**: 374–381.

Frey T. 1995. Nucleic acid dyes for detection of apoptosis in live cells. *Cytometry* **21**: 265–274.

Gage DJ, Bobo T, Long SR. 1996. Use of green fluorescent protein to visualize the early events of symbiosis between *Rhizobium meliloti* and alfalfa (*Medicago sativa*). *Journal of Bacteriology* **178**: 7159–7166.

Guindulain T, Comas J, Vives-Rego J. 1997. Use of nucleic acid dyes, SYTO-13, TOTO-1, and YOYO-1 in the study of *Escherichia coli* and marine prokaryotic populations by flow cytometry. *Applied and Environmental Microbiology.* **63**: 4608–4611.

Holmstrom TH, Chow SC, Elo I, Coffey ET, Orrenius S, Sistonen L, Eriksson JE. 1998. Suppression of Fas/APO-1-mediated apoptosis by mitogen-activated kinase signaling. *Journal of Immunology* **160**: 2626–2636.

Limpens E, Bisseling T. 2003. Signaling in symbiosis. *Current Opinion in Plant Biology* **6**: 343–350.

Limpens E, Franken C, Smit P, Willemse J, Bisseling T, Geurts R. 2003. LysM domain receptor kinases, regulating rhizobial Nod factor-induced infection. *Science* **302**: 630–633.

Mason DJ, Shanmuganathan S, Mortimer FC, Gant VA. 1998. A fluorescent gram stain for flow cytometry and epifluorescence microscopy. *Applied and Environmental Microbiology* **64**: 2681–2685.

Meade HM, Long SR, Ruvkun GB, Brown SE, Ausubel FM. 1982. Physical and genetic characterization of symbiotic and auxotrophic mutants of *Rhizobium meliloti* induced by Tn5 mutagenesis. *Journal of Bacteriology* **149**: 114–122.

Mylona P, Pawlowski K, Bisseling T. 1995. Symbiotic nitrogen fixation. *Plant Cell* **7**: 869–885.

Pulliam L, Stubblebine M, Hyun W. 1998. Quantification of neurotoxicity and identification of cellular subsets in a three-dimensional brain model. *Cytometry* **32**: 66–69.

Schultze M, Kondorosi A. 1998. Regulation of symbiotic root nodule development. *Annual Review of Genetics* **32**: 33–57.

Stougaard J. 2000. Regulators and regulation of legume root nodule development. *Plant Physiology* **124**: 531–540.

Trotta E, Paci M. 1998. Solution structure of DAPI selectively bound in the minor groove of a DNA T.T mismatch-containing site: NMR and molecular dynamics studies. *Nucleic Acids Research* **26**: 4706–4713.

Truchet G, Camut S, de Billy F, Odorico R, Vasse J. 1989. The *Rhizobium*–legume symbiosis. Two methods to discriminate between nodules and other root-derived structures. *Protoplasma* **149**: 82–88.

Vedam V, Haynes JG, Kannenberg EL, Carlson RW, Sherrier DJ. 2004. A *Rhizobium leguminosarum* lipopolysaccharide lipid-A mutant induces nitrogen-fixing nodules with delayed and defective bacteroid formation. *Molecular Plant–Microbe Interactions* **17**: 283–291.

Wilson KJ, Sessitsch A, Corbo JC, Giller KE, Akkermans ADL, Jefferson RA. 1995. Beta-glucuronidase (GUS) transposons for ecological and genetic studies of rhizobia and other gram-negative bacteria. *Microbiology – UK* **141**: 1691–1705.

Wood EA, Butcher GW, Brewin NJ, Kannenberg EL. 1989. Genetic derepression of a developmentally regulated lipopolysaccharide antigen from *Rhizobium leguminosarum* 3841. *Journal of Bacteriology.* **171**: 4549–4555.